Available online at www.sciencedirect.com
ScienceDirect
Mendeleev Commun., 2008, **18**, 305–306

Mendeleev
Communications

Photochemical reactions of trimethylene oxide radical cations in Freon matrices at 77 K

Mikhail Ya. Mel'nikov,* Vladilen N. Belevskii, Anastasiya D. Kalugina, Ol'ga L. Mel'nikova, Vladimir I. Pergushov and Daniil A. Tyurin

Department of Chemistry, M. V. Lomonosov Moscow State University, 119991 Moscow, Russian Federation.
Fax: +7 495 939 1814; e-mail: melnikov@excite.chem.msu.ru

DOI: 10.1016/j.mencom.2008.11.005

Radical cations of trimethylene oxide under photobleaching at 77 K could form either distonic radical cations $^{\bullet}CH_2CH_2CH{=}OH^+$/$^{\bullet}CH_2CH_2O^+{=}CH_2$ or oxetan-2-yl radicals depending on the Freon matrix used.

Radical cations (RCs) are the primary products of one-electron oxidation of organic molecules and act as intermediate particles in various processes in solids. The method of RC stabilization in low temperature Freon matrices[1] has been used extensively for the studies of the structure and reactivity of RCs in their ground and excited electronic states. It is known[2,3] that photolysis of RC of dimethyl ether and tetrahydrofuran in a Freon 11 matrix induces charge transfer to the matrix molecules, whereas photochemical reactions of the same RC in SF_6 and a Freon mixture (Freon 11/Freon 114B2) lead to their deprotonation.

The aim of this work was to study the mechanism and efficiency of the photochemical reactions of the RC of trimethylene oxide (TMO) stabilized in different Freon matrices at 77 K.

We used $CFCl_3$ (Freon 11, 99%, Aldrich), $CFCl_2CF_2Cl$ (Freon 113, 99.9%), CF_3CCl_3 (Freon 113a, 99%, Aldrich) as matrices; in certain cases, Freons were additionally purified using standard techniques. TMO (97%, Aldrich) was used without additional purification.

The solutions of TMO in Freons (0.1–0.5 mol%) evacuated at ~0.1 Pa were sealed in quartz and SK-4B glass tubes and irradiated with 2–4 kGy doses at 77 K. A 5BXV6-W X-ray generator (50 kV, 80 mA) was the emitting source.

The EPR spectra were recorded on a Varian E-3 X-band spectrometer. The concentration of paramagnetic centres in a sample was determined by comparison to the reference sample, a single crystal of $CuCl_2{\cdot}2H_2O$ with a known number of paramagnetic Cu^{2+} ions. The error in the absolute value of the concentration of paramagnetic species determined in this way did not exceed ±20%. Simulations of the EPR spectra were carried out with the use of the PEST WinSim and WINEPR Simfonia software.[4] Optical spectra were recorded on a Specord M-40 spectrophotometer at 77 K; quartz tubes with 1 mm optical path lengths were used for optical measurements. A DRSh-250 high-pressure mercury lamp with a glass filter to select mercury spectral lines at $\lambda = 546$ nm ($T_{max} = 35\%$, $\Delta\nu_{1/2} = 1800$ cm^{-1}) was used as a light source. The absolute light intensity measured by actinometry with Reinike salt was $5.8{\times}10^{-5}$ einstein cm^{-3} s^{-1}. Quantum yields were calculated from the dependences of the concentration of the RC and reaction products on the absorbed light dose; the error of the absolute values of the quantum yields determined in this way did not exceed ±25%.

Quantum chemical calculations were carried out using the spin-unrestricted density functional theory (DFT) with non-empirical hybrid functional PBE0.[5] We used core correlation consistent triple zet basis set Λ22.[6] To speed up the calculations, resolution-of identity techniques are used for the evaluation of Coulomb,[7] exchange and density-functional contributions.[8] Molecular geometries were fully optimized (tolerance on gradient: 10^{-5} a.u.). A very fine integration grid was used for the DFT exchange-correlation terms (accuracy of 10^{-8} a.u. per atom). A high accuracy solution of SCF equations was used (tolerance on density: 10^{-8} a.u.). The hyperfine splitting constants (hfcs) were evaluated from the spin density based electric field gradient tensors at nuclear positions using the point nucleus model. All calculations were done using the PRIRODA-04[9] program package.

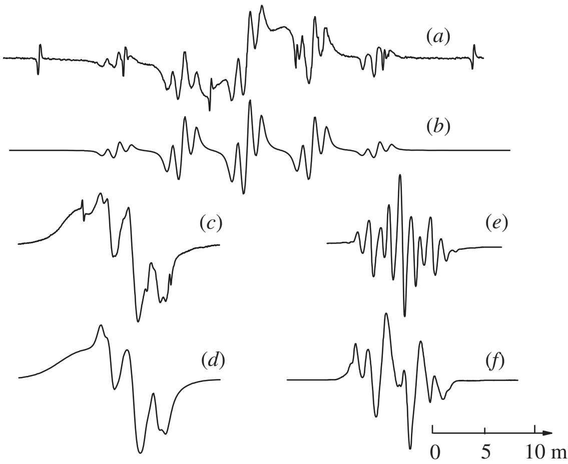

Figure 1 EPR spectra of the X-ray irradiated 0.1 mol% solutions of the TMO in Freon 113a: (*a*) at 77 K, (*b*) simulation with the following parameters: a(β-4H) = 6.5 mT, a(γ-2H) = 1.1 mT, (*c*) experimental spectrum after photobleaching (λ = 546 nm) at 77 K, (*d*) simulation of the spectrum of the distonic RC with $^{\bullet}CH_2CH_2$~ fragment, (*e*) after consequent annealing to 140 K; and (*f*) X-ray irradiated 2.5 mol% solutions of the TMO in Freon 11 at 150 K.

The EPR spectra of the X-ray irradiated 0.1 mol% solutions of TMO in Freon 113a at 77 K have a spectral pattern as a quintet of triplets [Figure 1(*a*)]. The central part of the EPR spectrum is distorted by the signal from the matrix and oxetan-2-yl radicals. The hfcs and g-tensor components were obtained from the modeling of the experimental EPR spectra [a(β-4H) = = 6.5 mT, a(γ-2H) = 1.15 mT, $g_{iso} \approx 2.010$] [Figure 1(*b*)]. These values are in good agreement with previous data[10] [a(β-4H) = = 6.4 mT, a(γ-2H) = 1.1 mT, $g_{iso} \approx 2.007$], and with the results of our quantum chemical calculations [a(β-4H) = 6.91 mT, a(γ-2H) = 1.28 mT].

The EPR spectra of the X-ray irradiated 0.1 mol% solutions of TMO in Freon 11 at 77 K also consist of a quintet signal with additional hyperfine structure. Angular dependence of the EPR spectra in this matrix observed at 77 K makes their interpretation more complicated. The hfcs obtained from the modeling of the experimental ESR spectra in Freon 11 are almost equal to the values given above for Freon 113a matrix.

The EPR spectra of the X-ray irradiated 0.1–0.5 mol% solutions of the TMO in Freon 113 at 77 K are similar to those observed in the Freon 11 and Freon 113a matrices. The larger line width obtained in Freon 113 if compared to the line width in Freon 11 and Freon 113a matrices, caused poor resolution of the hyperfine structure originating from two γ-protons in the EPR spectra of the TMO RC in Freon 113.

Photolysis (at 546 nm) of the TMO RC in Freon 11 and Freon 113a matrices at 77 K leads to the formation of new paramagnetic species [Figure 1(*c*)] with the conversion of more than 90%. The hfcs obtained from modeling of the observed EPR spectra [Figure 1(*d*)] are $a_{\text{iso}}(1\text{H}) = 2.08$ mT, $a_{\text{iso}}(1\text{H}) = 2.42$ mT and $a_{\text{iso}}(2\text{H}) = 0.72$ mT. The species formed under photolysis of the TMO RC in Freon 11 and Freon 113a matrices, after annealing of their frozen solutions at 140–150 K have identical EPR spectra with the spectral pattern of triplet of triplets [Figure 1(*e*)]. The temperature-dependent changes in the EPR spectra are totally reversible. The spectral pattern of the signal in the EPR spectra measured at 150 K allows us to assign the products of the reaction to the distonic RC with the fragment $\cdot CH_2CH_2\sim$. The hfcs, measured from the experimental EPR spectrum at 150 K, are $a(\alpha\text{-2H}) = 2.23$ mT, $a(2\text{H}) = 0.81$ mT, $g_{\text{iso}} \approx 2.003$ and are characteristic of this type of the RCs.[11] The quantum-chemical calculations have shown that the hfcs agree well with two types of species: conformers of the distonic RCs $\cdot CH_2CH_2O^+{=}CH_2$ [$a(\alpha\text{-2H}) = 2.39$ mT, $a(\beta\text{-2H}) = 0.57$ mT], and $\cdot CH_2CH_2CH{=}OH^+$ [$a(\alpha\text{-2H}) = 2.46$ mT, $a(\beta\text{-2H}) = 0.66$ mT]. The formation of $\cdot CH_2CH_2CH{=}OH^+$ occurs as a result of 1,2-migration of β-H atom to oxygen with the subsequent cleavage of the C–O bond. Note that the formation of these RCs is 75 kJ mol^{-1} more energetically favourable in the ground state than the formation of $\cdot CH_2CH_2O^+{=}CH_2$.

Photolysis (at 546 nm) of the X-ray irradiated 0.1 mol% solutions of TMO in Freon 11 at 77 K results in disappearance of two overlapping absorption bands with maxima at 450 and 300 nm in their optical spectra. The absorption band at 300 nm could be attributed to the absorption of the ionic pairs $CFCl_2\cdots Cl^-$, for which the absorption maximum at 310 nm has been reported previously.[12] At the same time, absorption at 430–460 nm is characteristic of the RC of the ethers.[2,3] The extinction coefficient was estimated from a relationship between absorbance at 450 nm and TMO RC concentration measured by EPR. The estimated value $\varepsilon_{\text{max}} \approx 3.2\times10^3$ dm^3 mol^{-1} cm^{-1} is in good agreement with data[2,3] for the RC of the ethers. The oscillator strength for the electronic transition ($f = 0.1$) was obtained from the formula[13] $f \cong 4.32\times10^{-9}\varepsilon_{\text{max}}\Delta\nu_{1/2}$, where ε_{max} is the molar absorption coefficient in the maximum of the absorption band, dm^3 mol^{-1} cm^{-1}; $\Delta\nu_{1/2}$ is the half-width of the absorption band, cm^{-1}.

Photolysis (at 546 nm) of the TMO RCs in the Freon 113 matrix at 77 K leads to the formation of TMO radicals. These radicals have a triplet signal in the EPR spectra with hfcs $a(2\text{H}) = 2.9$ mT. The formation of the same oxetan-2-yl radicals in 2.5 mol% solutions in Freon 11 is happening during X-ray irradiation at 77 K. Annealing of the X-ray irradiated 2.5 mol% solution of TMO in Freon 11 to 150 K causes a change of the EPR spectra to the triplet of doublets [$a(\alpha\text{-H}) = 0.9$ mT, $a(\beta\text{-2H}) = 2.9$ mT] [Figure 1(*f*)]. These temperature-induced changes are reversible. Our experimentally obtained hfcs are in good agreement with the ones [$a(\alpha\text{-H}) = 0.8$ mT, $a(\beta\text{-2H}) = 2.87$ mT] measured earlier[10] for oxetan-2-yl radicals, which were formed after annealing of the TMO RCs in Freon 113 to 110 K. The quantum-chemical calculated hfcs values [$a(\alpha\text{-H}) = 0.79$ mT, $a(\beta\text{-2H}) = 2.90$ mT] are in good agreement with the experimental data.

Table 1 Quantum yields (φ) of photochemical reactions of the TMO RC in Freon matrices.

Matrix	φ	Matrix	φ	Matrix	φ
Freon-11	0.4	Freon-113a	0.5	Freon-113	0.07

The quantum yields of the photochemical transformation of the TMO RCs, obtained from the dependence of the quantity of the reacted TMO RCs on the dose of light absorbed, are summarised in Table 1. These quantum yields are several times higher in the polycrystalline Freon 11 and Freon 113a matrices than in the glassy Freon 113 matrix. Therefore, the reaction leading to the formation of neutral radicals (1) is less effective if compared to the formation of the distonic RCs (2).

$$\text{cyclo-}C_3H_6O^{+\bullet} \rightarrow \text{cyclo-}C_3H_5O^{\bullet} + H^+ \qquad (1)$$

$$\text{cyclo-}C_3H_6O^{+\bullet} \rightarrow \cdot CH_2CH_2CH{=}OH^+/\cdot CH_2CH_2O^+{=}CH_2 \qquad (2)$$

It is possible that difference in the reaction pathways and efficiency of the RC transformations in different matrices could be explained by the fact that, in the polycrystalline matrices (Freon 11 and Freon 113a), the processes of the relaxation of the excited states are slower[14] than in the glassy Freon 113 matrix. Therefore, in the polycrystalline matrices, RCs undergo transformations in the non-relaxed vibrationally excited state. Different solvent surrounding RC in different Freon matrices[14] could also have some influence on the reaction pathways of the RC transformations and, in particular, on the reactions of their deprotonation.

This work was supported by the Russian Foundation for Basic Research (grant no. 07-03-00105) and the Presidium of the Russian Academy of Sciences (programme no. ChD-01).

References

1 T. Shida and T. Kato, *Chem. Phys. Lett.*, 1979, **68**, 106.

2 M. Ya. Mel'nikov, D. V. Baskakov, I. A. Baranova, V. N. Belevskii and O. L. Mel'nikova, *Mendeleev Commun.*, 1998, 2.

3 M. Ya. Mel'nikov, O. L. Mel'nikova, V. N. Belevskii and S. I. Belopushkin, *Khim. Vys. Energ.*, 1998, **32**, 57 [*High Energy Chem.* (*Engl. Transl.*), 1998, **32**, 34].

4 D. R. Duling, *J. Magn. Reson.*, 1994, **104B**, 105.

5 C. Adamo and V. Barone, *J. Chem. Phys.*, 1999, **110**, 6158.

6 D. N. Laikov, *Chem. Phys. Lett.*, 2005, **416**, 116.

7 O. Vahtras, J. Almlöf and M. W. Feyereisen, *Chem. Phys. Lett.*, 1993, **213**, 514.

8 D. N. Laikov, *Chem. Phys. Lett.*, 1997, **281**, 151.

9 D. N. Laikov and Yu. A. Ustynyuk, *Izv. Akad. Nauk, Ser. Khim.*, 2005, 804 (*Russ. Chem. Bull., Int. Ed.*, 2005, **54**, 820).

10 F. Williams and X.-Z. Qin, *Radiat. Phys. Chem.*, 1988, **32**, 299.

11 D. V. Baskakov, O. L. Melnikova, V. I. Feldman and M. Ya. Melnikov, *Khim. Vys. Energ.*, 2002, **36**, 138 [*High Energy Chem.* (*Engl. Transl.*), 2002, **36**, 103].

12 M. Ya. Melnikov, D. V. Baskakov and V. I. Feldman, *Khim. Vys. Energ.*, 2002, **36**, 346 [*High Energy Chem.* (*Engl. Transl.*), 2002, **36**, 309].

13 *Einführung in die Photochemie*, ed. G. O. Bekker, Deutscher Verlag der Wissenshaften, Berlin, 1976.

14 V. I. Feldman and M. Ya. Mel'nikov, *Khim. Vys. Energ.*, 2000, **34**, 279 [*High Energy Chem.* (*Engl. Transl.*), 2000, **34**, 236].

Received: 20th March 2008; Com. 08/3107